Dosage of amyloid precursor protein affects axonal contact guidance in Down syndrome

Lucas J. Sosa,[*,†] Nienke L. Postma,[*,†,1] Adriana Estrada-Bernal,[*,†,2] M. Hanna,[§,‖] R. Guo,[‡] Jorge Busciglio,[§,‖] and Karl H. Pfenninger[*,†,3]

[*]Department of Pediatrics and [†]Colorado Intellectual and Developmental Disabilities Research Center, School of Medicine, and [‡]Department of Biostatistics and Informatics, School of Public Health, University of Colorado, Aurora, Colorado, USA; and [§]Department of Neurobiology and Behavior and [‖]Institute for Memory Impairments and Neurological Disorders, University of California, Irvine, California, USA

ABSTRACT **Amyloid precursor protein (APP), encoded on Hsa21, functions as a cell adhesion molecule (CAM) in axonal growth cones (GCs) of the developing brain. We show here that axonal GCs of human fetal Down syndrome (DS) neurons (and of a DS mouse model) overexpress APP protein relative to euploid controls. We investigated whether DS neurons generate an abnormal, APP-dependent GC phenotype *in vitro*. On laminin, which binds APP and β1 integrins (Itgb1), DS neurons formed enlarged and faster-advancing GCs compared to controls. On peptide matrices that bind APP only, but not on those binding exclusively Itgb1 or L1CAM, DS GCs were significantly enlarged (2.0-fold), formed increased close adhesions (1.8-fold), and advanced faster (1.4-fold). In assays involving alternating stripes of monospecific matrices, human control GCs exhibited no preference for any of the substrates, whereas DS GCs preferred the APP-binding matrix (cross-over decreased significantly from 48.2 to 27.2%). Reducing APP expression in DS GCs with siRNA normalized most measures of the phenotype, including substrate choice. These experiments show that human DS neurons exhibit an APP-dependent, abnormal GC phenotype characterized by increased adhesion and altered contact guidance. The results suggest that APP overexpression may perturb axonal pathfinding and circuit formation in developing DS brain.—Sosa, L. J., Postma, N. L., Estrada-Bernal, A., Hanna, M., Guo, R., Busciglio, J., Pfenninger, K. H. Dosage of amyloid precursor protein affects axonal contact guidance in Down syndrome. *FASEB J.* 28, 195–205 (2014). www.fasebj.org**

Key Words: brain development · neurodevelopmental disorders

Down syndrome (DS), resulting from trisomy of Hsa21, is the most common cause of intellectual disability of known genetic etiology. However, the molecular and cellular mechanisms that cause the cognitive deficits are poorly understood. Among the many triplicate genes in DS is that encoding amyloid precursor protein (APP), a transmembrane glycoprotein known for its association with the pathogenesis of Alzheimer disease (1–4). Indeed, APP overdosage is believed to be responsible for the high incidence of early-onset Alzheimer disease in persons with DS. However, APP also is of great interest in development because of its high expression level in the developing CNS, and differentiating neurons in particular (5–9). Indeed, App-dependent endosomal abnormalities and impaired neuronal differentiation have been reported in the DS mouse model Ts65Dn (10–12). In rat brain, App also was found to be highly enriched in the axonal growth cone (GC), the leading edge of the growing axon (13). APP has been known for some time to interact with extracellular matrix (ECM) molecules (14–23) and to be involved in cell migration and neurite outgrowth (24–30), but its function as a cell adhesion molecule has been demonstrated only recently (31). These studies showed that the dosage of App protein significantly affects GC adhesion and spreading, even on a complex ECM component such as laminin, which contains distinct binding sites for both App and β1 integrin (Itgb1; also present in GCs; refs. 16, 32). Particularly important is the observation that App levels affect GC contact

Abbreviations: Abp, APP-binding peptide; APP, amyloid precursor protein; BSA, bovine serum albumin; CAM, cell adhesion molecule; DMEM, Dulbecco's modified Eagle's medium; DS, Down syndrome; ECM, extracellular matrix; eL1, L1 cell adhesion molecule outer domain; GC, growth cone; GCP, growth cone particle; Ibp, Itga3b1-binding peptide; Itg, integrin; Itgb1, β1 integrin; PBS, phosphate-buffered saline; RICM, reflection interference contrast microscopy; scrRNA, scrambled siRNA; siAPP, APP-targeted siRNA; TIRF, total internal reflection fluorescence; WT, wild-type

[1] Current address: Department of Child Neurology, VU University Medical Center, Amsterdam, The Netherlands.

[2] Current address: Department of Radiation Oncology, Ohio State University, Columbus, Ohio, USA.

[3] Correspondence: Department of Pediatrics, University of Colorado, Mailbox 8313, 12800 E. 19th Ave, Aurora, CO 80045, USA. E-mail: karl.pfenninger@ucdenver.edu

doi: 10.1096/fj.13-232686

guidance *in vitro* (31). As contact guidance is one of the mechanisms necessary for appropriate axonal pathfinding in the developing brain (33), defects in this mechanism are likely to result in miswiring of the brain and, thus, impairment of brain function, including cognitive deficit.

Our findings raised the questions of whether GCs of DS neurons exhibit a phenotype that might contribute to the neurodevelopmental deficits observed in DS, and to what extent such a phenotype depends on APP dosage. The present report addresses these questions in a series of *in vitro* studies with hippocampal neurons from the Ts65Dn mouse model of DS (34, 35) and, especially, with primary DS and euploid human fetal cortical neurons. It is important to consider that Ts65Dn mice are trisomic only for a subset of the genes located on Hsa21 (this includes the *APP* gene, however). Therefore, the analysis of human neurons is critical if we wish to understand brain development in the framework of the full complexity of human trisomy 21. The present studies show that, at least *in vitro*, DS neurons exhibit a significantly altered GC phenotype that includes perturbation of contact guidance.

MATERIALS AND METHODS

Materials

The primary antibodies used were: anti-N-terminal App (Sigma-Aldrich, St. Louis, MO, USA) and anti-Gap43 (AbCam, Cambridge, MA, USA) for blots; anti-C-terminal App (Epitomics, Burlingame, CA, USA), used for immunofluorescence.

The secondary antibodies used were anti-rabbit IgG conjugated with Alexa Fluor 647 (Cy5; for Western blot) and anti-rabbit IgG conjugated with Alexa Fluor 594 (red), from Cell Signaling Technology (Boston, MA, USA). Other fluorescent labels were phalloidin conjugated with Alexa Fluor 488 or 555 and Alexa Fluor 488- and 555-conjugated bovine serum albumin (BSA), from Molecular Probes (Eugene, OR, USA). To generate the monospecific culture substrates, we used peptides synthesized by GenicBio (Shenzhen, China). The sequence of the APP-binding peptide (Abp) was ARKQAASIKVAVS (16, 36). The Itga3b1-binding peptide sequence (Ibp) was PPFLMLLKGSTR (32).

The APP-targeted siRNAs (siAPPs) and the control scrambled siRNAs (scrRNAs) were obtained from Integrated DNA Technologies (Coralville, IA, USA). Their sequences were as follows (3 siRNAs were used together): NM_019288 duplex 1 5′-AGAAUCCAACAUACAAGUUCUUUGA-3′, NM_019288 duplex 2 5′-GCCAAAGAGACAUGCAGUGAGAAGA-3′, and NM_019288 duplex 3 5′-GUCAUAGCAACAGUGAUUGUCAUCA-3′. Control duplexes (DS ScrambledNeg; "scrambled") were sequences not present in the human, rat, or mouse transcriptomes.

Culture reagents and their sources were: Human laminin, from Sigma-Aldrich; mouse laminin, culture media, N2, and B27 supplements, Life Technology (Carlsbad, CA, USA). All other reagents were of the purest grade available and purchased from Sigma-Aldrich or Thermo-Fisher Scientific (Waltham, MA, USA).

Animals

The mice in this study [wild type (WT), C57BL/6J; Ts65Dn and their euploid littermates] were bred and maintained in an AAALAC-approved facility (Animal Welfare Assurance number PHS A3269-01). Breeders were obtained from The Jackson Laboratory (Bar Harbor, ME, USA). Mice were handled and humanely euthanized in compliance with protocol B21711(01)1E (approved by the University of Colorado Denver's Animal Care and Use Committee), the U.S. Public Health Service Policy on Humane Care and Use of Laboratory Animals, and the National Institutes of Health Guide for the Care and Use of Laboratory Animals.

Human neurons

Fetal human cortical brain samples (17–20 wk gestational age) were procured under protocols approved by the Internal Review Board of the University of California–Irvine. The protocols for obtaining fetal brain tissue comply with all federal and institutional guidelines, especially with respect to the confidentiality of the donor's identity. Written informed consent was obtained from all tissue donors. As the samples were obtained postmortem, are deidentified, and cannot be traced back to the donors, they have exempt status. Frozen tissue blocks were sent from the University of California–Irvine to the University of Colorado for the culture work (see below).

GC isolation

Mouse GC particles (GCPs) were isolated from individual brains following a protocol modified after previous reports (37, 38). Individual newborn mouse brains were homogenized in 450 μl of 0.32 M sucrose containing 1 mM $MgCl_2$, 2 mM TES buffer (2-[[1,3-dihydroxy-2-(hydroxymethyl)propan-2-yl]amino] ethanesulfonic acid), pH 7.3, and 2 μM aprotinin (all procedures at 4°C). The homogenate was placed in 0.6-ml tubes in a SW55Ti rotor (Beckman Coulter, Fullerton, CA, USA) and spun for 10 min at 1092 g_{av}. The resulting low-speed supernatant (LSS; 0.4 ml) was layered onto 0.2 ml of 0.83 M sucrose containing 1 mM $MgCl_2$ and 2 mM TES and centrifuged in a TLA-120.2 rotor (Beckman Coulter) for 12 min at 244,632 g_{av} (acceleration 5 min, deceleration 7 min). The band containing the GCPs was recovered from the interface and diluted in 0.32 M sucrose to a final volume of 1.5 ml. The samples were spun in a JA-18.1 rotor (Beckman Coulter) for 45 min at 37,480 g_{av}. The supernatant was discarded, and the pellet (GCPs) was resuspended in 20 μl of 0.32 M sucrose for protein analysis and electrophoresis.

Gel electrophoresis and Western blot

Samples were resolved by SDS-polyacrylamide gel electrophoresis and transferred onto polyvinylidene fluoride (PVDF) membranes (Millipore, Billerica, MA, USA). Blots were blocked with 5% nonfat milk and 0.1% Tween-20 in Tris-buffered saline (TBS) for at least 1 h, incubated with primary antibody for 1 h (room temperature), washed with TBS-Tween-20 3 times, incubated with Cy5 fluorophore-conjugated secondary antibody for 1 h, and washed. Bound antibody was quantified in a laser fluorescence scanner (Typhoon 9400; GE Healthcare, Piscataway, NJ, USA).

Cell culture and transfection

Cultures of human cortical neurons were prepared essentially as described previously (39): Frozen tissue blocks were thawed by transferring the vial content (1.5–2 ml) to 50 ml of Hank's balanced salt solution (HBSS) at 37°C in order to remove DMSO. The tissues were retrieved from the bottom of

the conical tube, placed in 10 ml HBSS with 400 μl of 0.25% trypsin (Life Technology) and incubated for 2 × 5 min at 37°C, the second time with gentle agitation. The tissues were washed with 10 ml of Dulbecco's modified Eagle's medium (DMEM) for 5 min and then dissociated gently with a wide-orifice pipette tip in 10 ml DMEM plus N2 supplement. For some experiments, dissociated DS neurons were transfected prior to plating with siAPP (0.3 nM each of 3 sequences), or control scrRNA, plus 0.7 μg pmaxGFP vector to label transfected cells (Lonza Group, Basel, Switzerland) in 100 μl. Transfection was by electroporation, using the optimized Amaxa Nucleofector (Lonza Group) protocol (OO3). For these studies, we used cortical neurons from 10 euploid and 11 DS fetus. Dissociated hippocampal mouse neurons were obtained from newborn mice. Pups were karyotyped to identify Ts65Dn and euploid littermates (which served as control) before setting up the cultures.

Uniform culture substrates and media

The dissociated human and mouse neurons were plated onto laminin-, peptide-, or L1 cell adhesion molecule (CAM) outer domain (eL1)-coated glass coverslips (Assistent Brand; Carolina Biological Supply, Burlington, NC, USA). Synthetic culture substrates were prepared by coating 25-mm coverslips with 10 μg Abp or Ibp or with 2.85 μg eL1 as described previously (31). The mouse and human neurons plated on laminin were maintained in DMEM plus N2 and B27 supplements, without serum (40). For the culture of the human neurons on the synthetic matrices, we used only the N2 supplements, but without putrescine in order to avoid nonspecific cell adhesion to the substrate.

Substrate choice assays

Striped matrices of paired Abp, Ibp, or eL1 were made essentially as described previously (31, 41, 42). After placing the silicone "stamp" (consisting of alternating, 55/45-μm-wide bars and channels) onto the coverslip, the first peptide solution [75 μM in phosphate-buffered saline (PBS)] was infused and incubated for 1 h at 37°C. To mark the first set of stripes, we incubated them with Alexa Fluor 488-BSA or 555-BSA (150 nM) for 1 h at 37°C, before blocking them with 1% (w/v) BSA in PBS for 30 min at 37°C. To establish the second set of lanes, we removed the stamp and added the second peptide (75 μM). The eL1 substrate was deposited in the same manner, at a concentration of 10 μg/ml. After incubation for 1h at 37°C, we washed and blocked the matrices with 1% BSA in PBS for 30 min at 37°C. Thereafter, dissociated neurons were deposited on these matrices and allowed to grow for 2 d in N2 medium before fixation and processing for microscopy. The axonal substrate preference was assessed quantitatively with the border zone analysis (31).

Cell labeling and microscopy

Cells were fixed using slow infusion of 4% (w/v) formaldehyde in 0.1 M phosphate buffer (pH 7.4) with 120 mM glucose and 0.4 mM $CaCl_2$ for a total of 30 min (43). Cultures were rinsed with PBS containing 1 mM glycine, permeabilized for 2 min with 1% (v/v) Brij98 detergent in blocking buffer (PBS with 1% w/v BSA) and placed in blocking buffer for 1 h. Cultures were incubated with primary antibody for 1 h, washed with blocking buffer (3×), labeled with Alexa Fluor 594-conjugated secondary antibodies (1 h), and washed before embedding in Fluoromount-G reagent (Southern Biotech, Birmingham, AL, USA). Some samples were incubated with Alexa Fluor 488 or 555-phalloidin conjugate to label filamentous actin. These procedures were performed at room temperature.

Images were acquired with a Zeiss Axiovert 200M microscope with Zeiss optics (objectives: ×40 Fluar ×40/1.3; Plan-Apo ×63/1.4; Alpha Plan-Apo ×100/1.46; Carl Zeiss, Oberkochen, Germany) and Cooke Sensicam camera (Cooke Corp., Romulus, MI, USA), controlled by μManager software (44). To acquire reflection interference contrast microscopy (RICM) images (45), live cultures were placed in an open chamber with medium, layered over with inert mineral oil, and examined under convective heating. Close adhesions were quantified using thresholding and area measurement (Metamorph software, Molecular Devices, Sunnyvale, CA, USA; ref. 46). For total internal reflection fluorescence (TIRF) microscopy, cells were examined with the ×100/1.46 objective, in combination with an argon/krypton laser-coupled TIRF illuminator (Zeiss).

Statistical analysis

Student's 2-sample *t* test was used to examine the statistically significant difference for 2-group comparisons as previously reported for essentially the same assays (31). For comparisons with >2 groups, unbalanced 1-way analysis of variance (ANOVA), followed by its *post hoc* pairwise comparisons, or planned contrast analysis with appropriate correction for multiple comparisons were performed to study the group differences. More specifically, unbalanced ANOVA followed by *post hoc* Tukey-Kramer test was performed for the comparisons of Ts65Dn, euploid and WT. For the comparisons involving euploid, DS, DS+siAPP, and DS+scrRNA on Abp, we conducted unbalanced ANOVA followed by planned contrast analysis (euploid *vs.* DS, euploid *vs.* DS+siAPP, DS *vs.* DS+siAPP, and DS+siAPP *vs.* DS+scrRNA for analysis of GC area, APP intensity, number of filopodia and axon length; euploid *vs.* DS, euploid *vs.* DS+siAPP, DS *vs.* DS+siAPP, DS *vs.* DS+scrRNA, and DS+siAPP *vs.* DS+scrRNA for analysis of contact guidance). The resulting *P* values were adjusted for multiple comparisons using the Bonferroni method. All *P* values presented are based on 2-sided tests.

RESULTS

App level and phenotype of Ts65Dn GCs on laminin

Axonal GCs can be isolated by subcellular fractionation from developing rodent brain for biochemical analysis (37). Like in rat brain (13), App is highly enriched in such GCPs of the mouse brain, at least as much as the GC marker protein Gap43 (**Fig. 1*A***). Using GCP isolation and quantitative analysis of Western blots, we determined that App protein was increased ~1.7-fold in Ts65Dn GCs compared to those from euploid littermates ($P < 0.0001$; Fig. 1*A*). These data suggested that, on App-binding matrices, such as laminin, Ts65Dn neurons and, especially, their GCs should be more spread out and adherent. This property was analyzed by phase-contrast microscopy and RICM, a well-established method for imaging the reduced cell-substrate gap characteristic of cellular adhesive structures or "close adhesions" (45, 47–49). When hippocampal neurons from Ts65Dn mice were

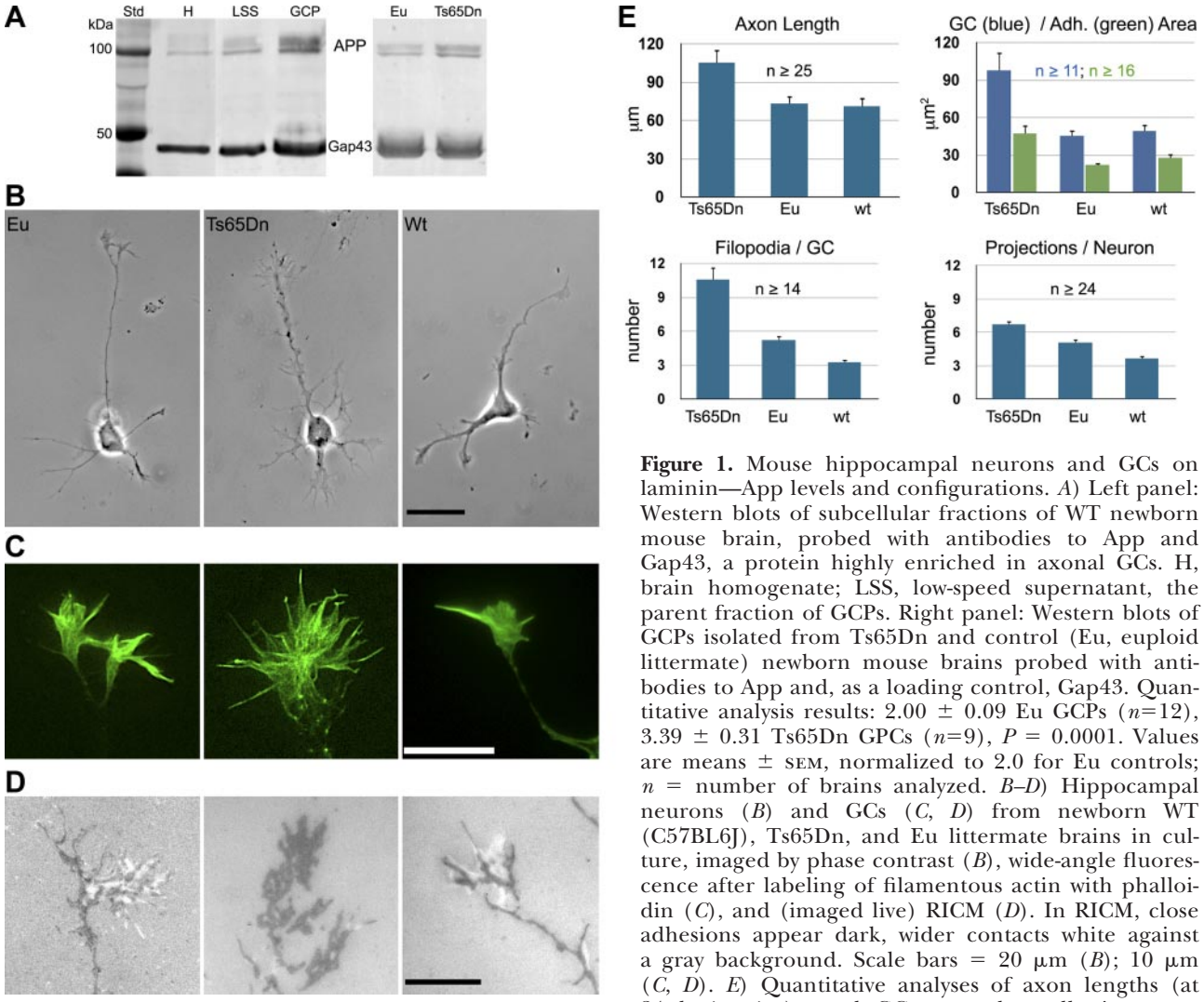

Figure 1. Mouse hippocampal neurons and GCs on laminin—App levels and configurations. *A*) Left panel: Western blots of subcellular fractions of WT newborn mouse brain, probed with antibodies to App and Gap43, a protein highly enriched in axonal GCs. H, brain homogenate; LSS, low-speed supernatant, the parent fraction of GCPs. Right panel: Western blots of GCPs isolated from Ts65Dn and control (Eu, euploid littermate) newborn mouse brains probed with antibodies to App and, as a loading control, Gap43. Quantitative analysis results: 2.00 ± 0.09 Eu GCPs (n=12), 3.39 ± 0.31 Ts65Dn GPCs (n=9), P = 0.0001. Values are means ± SEM, normalized to 2.0 for Eu controls; n = number of brains analyzed. *B–D*) Hippocampal neurons (*B*) and GCs (*C*, *D*) from newborn WT (C57BL6J), Ts65Dn, and Eu littermate brains in culture, imaged by phase contrast (*B*), wide-angle fluorescence after labeling of filamentous actin with phalloidin (*C*), and (imaged live) RICM (*D*). In RICM, close adhesions appear dark, wider contacts white against a gray background. Scale bars = 20 µm (*B*); 10 µm (*C*, *D*). *E*) Quantitative analyses of axon lengths (at 24 h *in vitro*), total GC area, close-adhesion area, number of filopodia/GC, and unidentified projections/neuron. See Table 1 for P values obtained by ANOVA *post hoc* Tukey-Kramer test. n = number of neurons analyzed from ≥3 mice.

grown on laminin, their GCs were significantly larger, formed larger adhesive areas (as seen by RICM) and advanced faster compared to those from euploid littermates or WT mice (Fig. 1*B–E* and **Table 1**). [Because of the complex genetic background of the Ts65Dn mice (50), the appropriate controls are euploid littermates. However, to allow for comparison with data from commonly used WT mice, we also show results from C57BL6J mice]. The Ts65Dn neurons were further characterized by an abundance of appendages of variable size and shape. In GCs, they were readily identifiable as filopodia, but on parikarya, axon shafts, and dendrites, they were difficult to distinguish from emerging neurites, neurite branches, or filopodial/lamellipodial structures. Therefore, we refer to them as unidentified projections. They were significantly more numerous in Ts65Dn neurons than those on euploid littermate and WT neurons. Overall, these results showed that developing Ts65Dn neurons and GCs exhibited an abnormal phenotype on laminin *in vitro*. Because of the important neurodevelopmental implications of this observation, we proceeded to analyze the phenotype of primary human DS neurons *in vitro*.

APP level and phenotype of DS neurons on laminin

It was not feasible to isolate human GCs for biochemical analysis. Therefore, we assessed APP levels in DS GCs by immunolabeling combined with TIRF microscopy. TIRF microscopy chiefly images the substrate-facing plasma membrane of cells, because excitation of fluorophores by the evanescent wave is effectively limited to a sample depth of ~150 nm. Therefore, the TIRF GC images reveal primarily plasmalemmal APP, with only minimal signal contribution by internal membrane compartments. As shown in **Fig. 2**, APP fluorescence intensity in the adherent plasma membrane of DS GCs on laminin was increased about 8-fold relative to that of euploid GCs, indicating a significant increase in surface APP. This is consistent with previous results

TABLE 1. *Adjusted* P *values obtained by ANOVA with* post hoc *Tukey-Kramer test*

Parameter	Ts65DN	WT
Axon length		
Euploid	0.0096	0.98
WT	0.0059	
GC area		
Euploid	0.0003	0.93
WT	0.0002	
Adhesion area		
Euploid	0.0005	0.58
WT	0.0045	
Filopodia/GC		
Euploid	<0.0001	0.035
WT	<0.0001	
Projections/neuron		
Euploid	0.0012	0.0065
WT	<0.0001	

See Fig. 1*E*.

that APP levels are well above the predicted dosage in DS neurons (51). The DS GCs were greatly enlarged, advanced faster (axon length after 48 h in culture) and were richer in filopodia than their euploid controls (Fig. 2). Neuronal perikarya exhibited an increased number of unidentified projections, and axons were broadly attached, with an abundance of such projections. Thus, the human DS GCs were distinct from their euploid controls and similar to those from Ts65Dn mice.

Analysis of DS GC adhesions

To study the adhesions of DS GCs in detail, we grew these neurons on monospecific matrices, laminin-derived peptides that bound only APP (Abp; ref. 16) or Itgb1s (Ibp; ref. 32), or the L1 CAM (eL1; ref. 52). These matrices supported normal survival and outgrowth of mouse cortical and hippocampal neurons *in vitro* (31). Euploid human cortical neurons also grew normally and formed close adhesions on these synthetic matrices.

We measured the relative APP fluorescence intensities of euploid *vs.* DS GCs on Abp using TIRF images. The average difference was not as great as on laminin but still a significant 2.3-fold (**Fig. 3*C*** and **Table 2**). Comparisons of axon outgrowth, GC configuration, and GC close adhesion of DS and euploid neurons on the different synthetic matrices are shown in Fig. 3*A*. The images and quantitative analyses (Fig. 3*C* and Table 2) indicated that DS neurons exhibited a distinctive phenotype, including enhanced GC spreading, significantly enlarged close adhesive area, and increased axon length (in 48 h), on Abp but not on the other matrices. The number of GC filopodia also was increased in DS *vs.* euploid neurons, but this phenomenon was not strictly substrate dependent. On Ibp and eL1 filopodial numbers of DS GCs were increased significantly com-

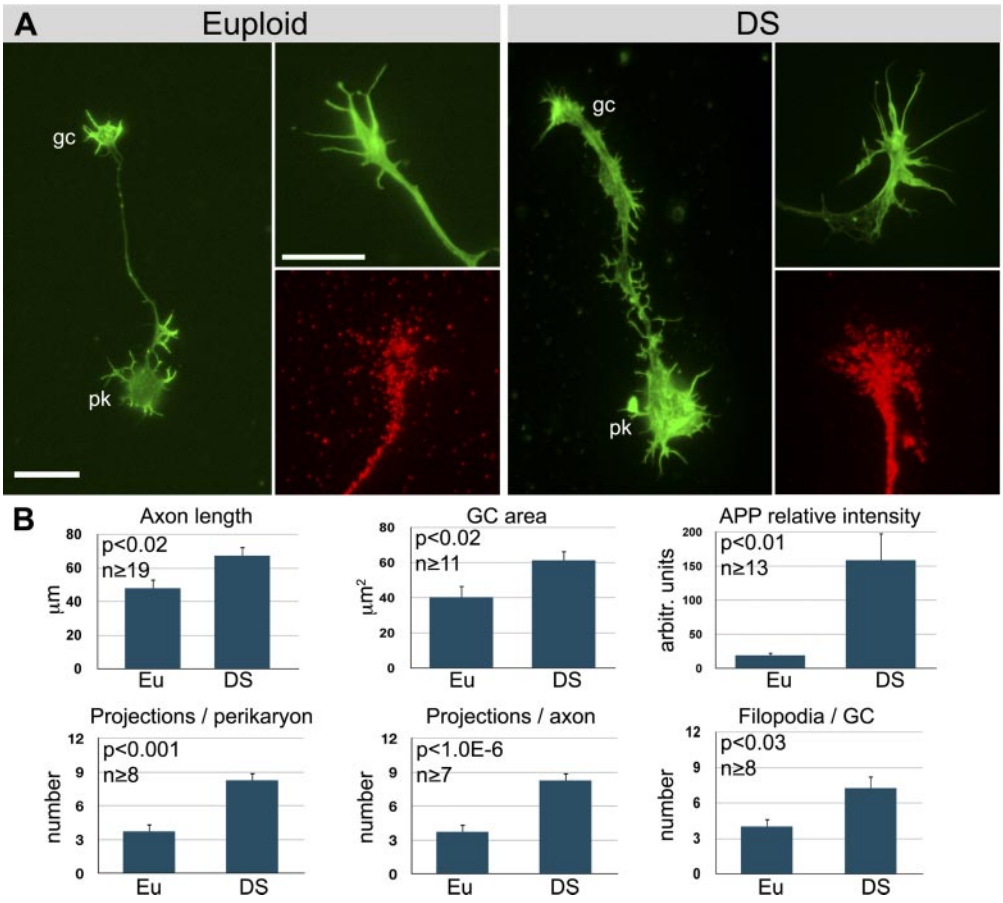

Figure 2. Human cortical neurons on laminin. *A*) Dissociated cortical neurons from healthy (euploid) and DS fetus as seen after palloidin labeling (green) of filamentous actin (whole neuron, left; GC detail, top right), and after labeling with anti-APP (red) and imaged by TIRF microscopy. pk, perikaryon; gc, axonal GC. Scale bars = 20 µm (whole neuron); 10 µm (GC detail). *B*) Results of morphometric analyses. Axon length, measured at 48 h *in vitro*; GC area, total spread area; projections per perikaryon or axon, number of unidentified projections. *P* values were obtained by Student's *t* test. *n* = number of neurons analyzed from ≥3 samples.

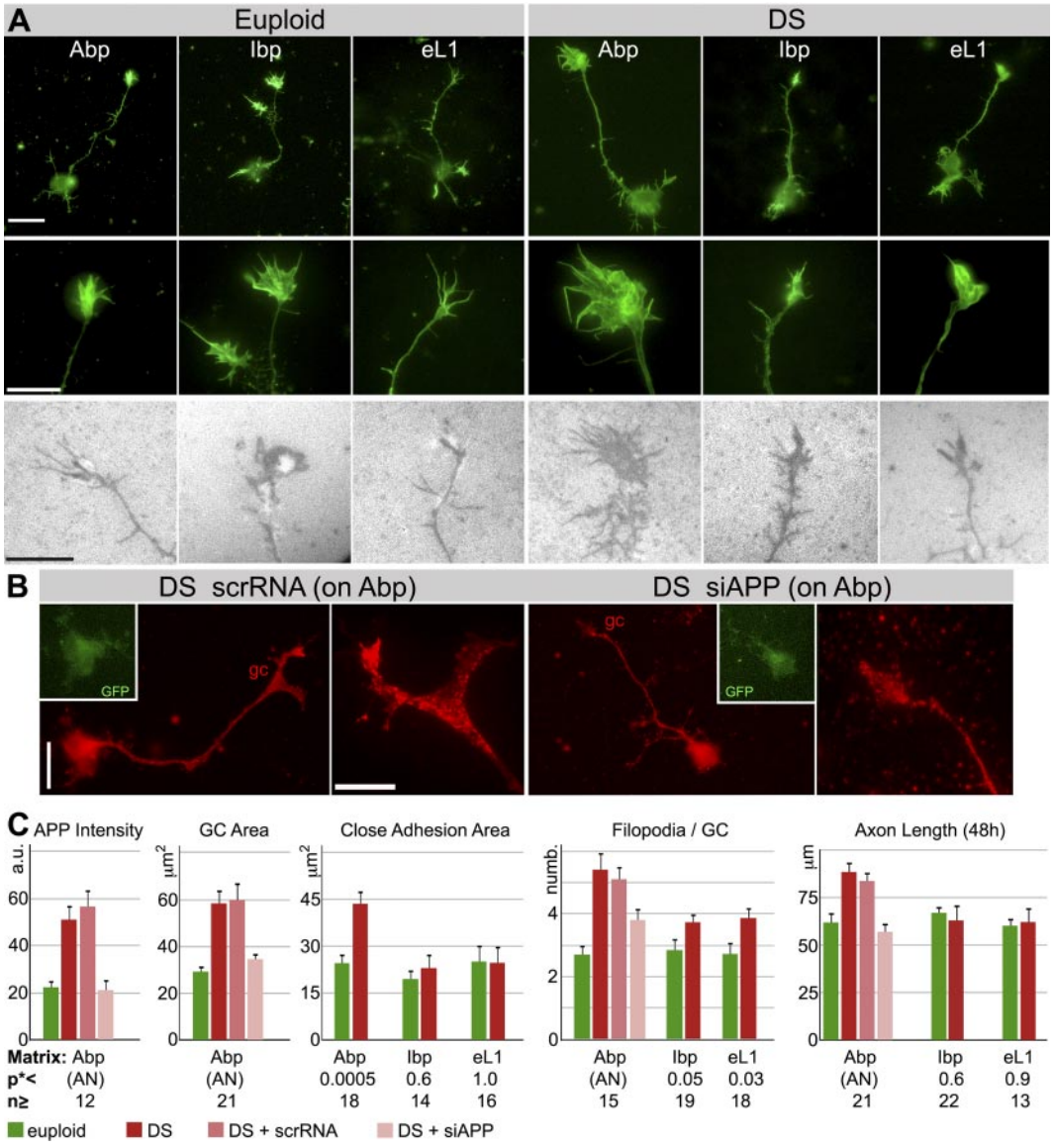

Figure 3. Dissociated euploid and DS human cortical neurons on monospecific, synthetic matrices. *A*) Phalloidin-labeled (green) whole neurons (top panels) and their GCs (middle panels), and RICM images of live GCs (bottom panels). Scale bars = 20 μm (top panels); 10 μm (middle and bottom panels). *B*) DS neurons and their GCs on Abp. Neurons were transfected with control scrRNA or siAPP (rescue experiment) and labeled with anti-APP (red; TIRF). GFP, transfection marker in perikaryon. Scale bars = 20 μm (whole neuron); 10 μm (GC detail). *C*) Results of morphometric analyses. a.u., arbitrary units (APP intensity, determined in TIRF images). See Table 2 for *P* values obtained by planned contrast analysis of ANOVA (AN; adjusted for multiple comparisons).*P values obtained by Student's t tests, together with n values (number of neurons analyzed from ≥3 samples), are shown below bar graphs.

pared to control GCs, but they did not reach the level of DS GCs on Abp (Fig. 3*A*, *C* and Table 2). Overall, however, our results suggested that APP played a significant and important role in the generation of the DS neuron phenotype, especially GC adhesion, spreading and axon elongation.

Based on these observations we decided to reduce APP expression by siRNA transfection in DS neurons growing on Abp in order to test whether the normal GC phenotype could be restored in these neurons. Transfection with the scrRNA control did not seem to affect any of the measured parameters. The partial reduction of APP expression in DS neurons, as determined by TIRF microscopy, is shown in Fig. 3*B*, *C* and resulted in an average GC APP level that was indistinguishable from euploid controls. Axon length (after 48 h) and GC area of such neurons were significantly reduced compared to those of DS neurons transfected with scrambled siRNA and not different from euploid controls. Treatment with siAPP also reduced the number of GC filopodia significantly compared to nontransfected DS controls. However, the DS + siAPP value was statistically indistinguishable from both the DS + scrRNA control and the euploid neurons. This implied that siRNA-induced return to euploid level was not com-

TABLE 2. *Adjusted* P *values obtained by planned contrast analysis of ANOVA*

Parameter	Euploid	DS	DS + scrRNA
APP intensity			
Euploid		0.039	
DS + siRNA	1.00	0.010	<0.0001
GC area			
Euploid		0.0007	
DS + siRNA	1.00	0.0097	0.0027
Filopodia			
Euploid		<0.0001	
DS + siRNA	0.15	0.043	0.14
Axon length, 48 h			
Euploid		0.0016	
DS + siRNA	1.00	<0.0001	0.0024

See Fig. 3*C*. Values are adjusted for multiple comparisons.

plete, as suggested by the bar graph in Fig. 3 (also note that the DS+siAPP value on Abp corresponds to the DS values on Ibp and eL1). Together with the fact that these filopodia were not completely substrate (Abp) dependent, this result suggested the involvement of other genes. Aside from GC filopodia, however, partial APP knockdown restored the normal phenotype in DS neurons in these experiments on Abp.

Contact guidance of human cortical axons *in vitro*

GC contact guidance plays an important role in the establishment of neuronal networks in the developing brain. To test GCs for differences in substrate preference, we prepared culture matrices consisting of stripes of alternating substrates (one of them quenched with fluorescent BSA for identification; ref. 31) and plated the human neurons on them. For quantitative analysis, we focused on two border zones, 5 μm wide, on either side of the interfaces between the substrates. Once within these zones, the GCs (~5 μm diameter) could detect the juxtaposed matrix and thus choose between the substrates. For each axon, we measured the cumulative length grown in the juxtaposed border zone as a percentage of the total combined lengths grown in both border zones (31). Thus, 50% crossover meant that there was no preference for either substrate. We found that euploid GCs had no preference for any one of the 3 substrates, and that the DS GCs did not favor either substrate in an eL1 *vs.* Ibp comparison (**Fig. 4** and **Table 3**). However, in the Abp *vs.* Ibp juxtaposition, DS GCs significantly favored Abp over Ibp. Therefore, DS GCs exhibited abnormal contact guidance in a comparison that involved an APP-binding substrate.

We also tested whether partial APP knockdown (see Fig. 3*B, C* and Table 2) restored the normal contact guidance phenotype in DS neurons. DS neurons transfected with the scrRNA sequence were indistinguishable from nontransfected DS neurons in Abp → Ibp juxtapositions; *i.e.*, they also showed preference for Abp (Fig. 4 and Table 3). On transfection with siAPP and reduction of GC APP levels to euploid, however, DS neurons lost this substrate preference and behaved like euploid neurons.

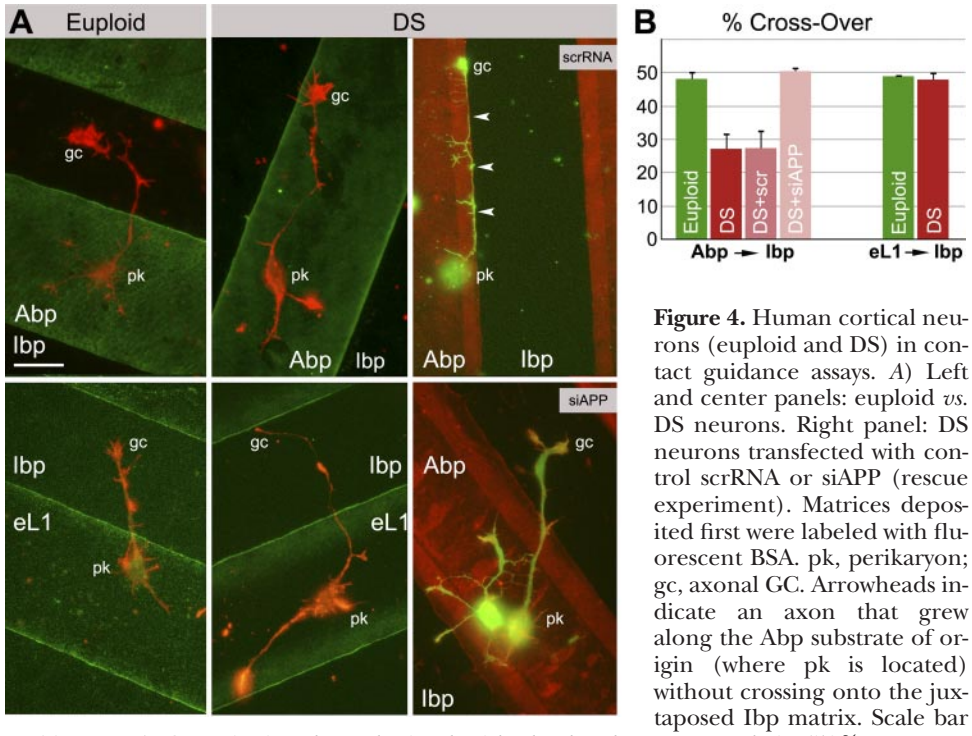

Figure 4. Human cortical neurons (euploid and DS) in contact guidance assays. *A*) Left and center panels: euploid *vs.* DS neurons. Right panel: DS neurons transfected with control scrRNA or siAPP (rescue experiment). Matrices deposited first were labeled with fluorescent BSA. pk, perikaryon; gc, axonal GC. Arrowheads indicate an axon that grew along the Abp substrate of origin (where pk is located) without crossing onto the juxtaposed Ibp matrix. Scale bar = 20 μm. *B*) Quantitative data obtained with the border zone analysis (50% crossover indicates no substrate preference; reduced crossover means preference for the substrate of origin, *i.e.*, Abp for left set of bars. See Table 3 for adjusted *P* values for Abp → Ibp and eL1 → Ibp experiments. *n* = number of neurons analyzed from ≥3 samples.

TABLE 3. *Adjusted* P *values for Abp → Ibp experiment, obtained by planned contrast analysis of ANOVA, and eL1 → Ibp experiment, obtained by Student's* t *test*

Experiment	Euploid	DS	DS +scrRNA
Abp → Ibp, ANOVA, $n \geq 16$			
DS	0.0011		1.00
DS + siAPP	1.00	0.0001	0.0004
eL1 → Ibp, Student's *t* test, $n \geq 25$			
DS	0.67		

See Fig. 4*B*.

DISCUSSION

Overexpression of APP in DS GCs

It has been known that App/APP is overexpressed in the brains of Ts65Dn mice, DS subjects (35, 53–57), and DS cortical neurons in culture (51), but no data were available on GCs. Our data show that the total amount of App protein is significantly increased in axonal GCs of Ts65Dn neurons compared to those of euploid littermates. The elevated (1.7-fold) protein level is slightly above what one would expect on the basis of gene dosage alone. We do not know, however, what fraction of the APP detected by Western blot is in the plasma membrane. Our microscopic analysis of human GCs labeled with APP antibody showed that the TIRF signal of the GC's adhesive plasma membrane was increased about 8-fold on laminin and ~2.3-fold on Abp compared to euploid controls. We do not know why these numbers differed, and why they were greater than the increase measured by Western blot in the isolated mouse GCs. Species differences and nonlinearity of the measurements are possible explanations. More likely, however, are the possibilities that APP clustering at the adhesions (known to occur; see ref. 31) increases the signal detected by TIRF; the majority of overexpressed APP is inserted into the plasmalemma rather than contained in internal compartments; and the endocytic pathway, and thus internalization of APP, is impaired (58) in DS neurons. In fact, all explanations may apply to some degree. In any case, the important result in the present context is that the TIRF measurements demonstrated a significant increase in APP expression in DS GCs. This observation prompted our hypothesis that both the DS GC and its mouse model counterpart exhibit a phenotype comprising some of the characteristics of GCs overexpressing APP alone.

We observed that on the physiological substrate laminin, which binds both App/APP and Itgb1s (16, 32), Ts65Dn mouse, and human DS GCs of hippocampal and cortical neurons, respectively, are enlarged, exhibit increased close-adhesion areas, bear an increased number of filopodia, and advance faster compared to euploid controls. Indeed, these differences constitute a distinctive phenotype for the Ts65Dn and DS growing neurons that resembles growing mouse hippocampal neurons overexpressing APP alone (31).

Spreading, substrate adhesion, and advance of DS GCs

To examine GC adhesion of human neurons in greater detail, we grew them on monospecific growth substrates. In contrast to euploid neurons, DS cortical neurons formed very large and strongly adhesive GCs on Abp. On Ibp and eL1, however, DS neurons formed axonal GCs that were almost identical to those of euploid neurons. This property of the DS GCs was very similar to that of GCs overexpressing APP alone (31). Therefore, enhanced adhesion and spreading of DS GCs were dependent on the level of APP protein. This conclusion was confirmed by partial APP knockdown in DS neurons using siAPP. The resulting APP protein level in such GCs, as assessed for the adhesive plasma membrane using TIRF microscopy, was reduced but not eliminated and very similar to that of euploid GCs. This normalization of APP protein did indeed reduce GC area to that found in euploid human neurons on the Abp substrate. It follows from these experiments that DS GCs exhibit an abnormally spread-out and adhesive phenotype that depends, at least to a large degree, on the increased *APP* gene dosage and the resulting overexpression of the adhesion molecule APP.

The Ts65Dn and DS GCs advanced more rapidly than their controls on laminin as judged from the axon lengths after the first 24 or 48 h *in vitro*. The same observation was made for DS neurons on Abp, but not on Ibp and eL1, indicating that increased axon growth of these neurons was dependent on APP-mediated cell adhesion. Yet, in our earlier experimentation (31) the axons of APP-overexpressing neurons grew more slowly on Abp compared to control axons. As we explained, amoeboid cell motility (a process analogous to GC advance) depends on cell adhesion in bimodal fashion, with motility decreased below and above an optimum level of adhesion (59–61). In the previous studies, the GC level of App/APP protein (as determined by Western blot) in APP-overexpressing neurons was nearly 2× that of WT (31) whereas, in the Ts65Dn GCs, it was only 1.7× control. Thus, the increased App/APP dosage in the former neurons and GCs may explain reduced outgrowth. It is possible that trisomy of other genes in DS neurons may have contributed to accelerated outgrowth, but this seems not likely, because partial knockdown of APP in DS neurons restored the normal outgrowth rate.

Appendages of DS axons

The use of monospecific growth substrates allowed examination of neuron and GC features that depended on a single type of adhesion molecule. As on laminin, the DS neurons grown on Abp formed strikingly abundant GC filopodia and unidentified projections (on

neurite shafts and perikarya). Interestingly, however, a significant increase in the number of these appendages in DS neurons was observed on the Ibp and eL1 matrices as well. Furthermore, the increased numbers of filopodia on GCs were not found in neurons overexpressing APP alone (31), and they seemed to persist to some extent on DS neurons after partial APP knockdown. These results indicated that APP-mediated cell adhesion contributed to, but was not necessary for, increased formation of filopodia. Therefore, the participation of other trisomic genes was likely. An obvious candidate was *TIAM1* (T-lymphoma invasive and metastasis-inducing 1) located on Hsa21, which encodes a guanine nucleotide exchange factor that activates the Rho family members Rac1 and Cdc42 (54, 62, 63).

4. Contact guidance of DS GCs is perturbed

The guidance of growth cones to their target areas depends on diffusible (attractants, repellents) as well as substrate-bound factors (33). The stripe assays used here have been developed to assess quantitatively the substrate preference or contact guidance of growing axons (41, 64). As shown previously, the level of APP expression in the axon profoundly affects GC discrimination among APP-binding and nonbinding matrices (31). Our current findings indicate that these effects also apply to DS GCs. Like those overexpressing APP alone, DS GCs behaved like euploid GCs on Ibp or eL1, but, in contrast to euploid GCs, they greatly preferred Abp over Ibp. Partial knockdown of APP in DS GCs restored the euploid behavior in these assays. These observations are important because they establish that DS GCs can make aberrant pathfinding decisions that might affect the development of the brain's circuitry.

CONCLUSIONS

The difficulty of determining the mechanisms by which human trisomy 21 causes cognitive disability rests largely on the plethora of genes that may contribute to the syndrome. Consequently, there is no "DS gene" whose increased dosage causes the cognitive deficiencies of DS. Yet, APP has been of great interest because most individuals with DS develop an early-onset form of Alzheimer disease. For the present report, however, we investigated the role of APP in brain development.

This study shows that DS neurons and, especially, their axonal GCs exhibit a distinctive phenotype dependent primarily on the overexpression of APP and the resulting increase in GC adhesion. Interestingly, however, the excessive formation of filopodia and other appendages, another aspect of this phenotype, was not entirely APP dependent and indicated the contribution of other genes. The results reported here were obtained *in vitro* and, to a large extent with mono-specific culture substrates. However, the GC phenotype observed on the laminin-derived Abp was present also on laminin (a brain ECM protein), even though laminin is a major Itgb1 substrate. Thus, it is highly likely that APP overexpression also affects GC function in the more complex microenvironment of the developing brain *in vivo*. Thus, our experiments may have uncovered a GC-based mechanism that contributes to the pathogenesis of DS-associated intellectual disability, an hypothesis that remains to be tested. FJ

The authors thank Dr. Katheleen Gardiner for reviewing the manuscript and for many helpful discussions; Drs. Ken Maclean and Hua Jiang for their assistance with breeding and genotyping Ts65Dn mice; Dr. Martin Grumet (Rutgers W. M. Keck Center for Collaborative Neuroscience, Piscataway, NJ, USA) for the generous gift of eL1 recombinant protein; and Carmel Harberg for excellent assistance with the preparation of the manuscript. This research was supported by grants from the U.S. National Institutes of Health (NIH)/National Institute of Neurological Disorders and Stroke (R01 NS061940), the Anna and John J. Sie Foundation (Denver, CO, USA), the Linda Crnic Institute for Down Syndrome (Denver, CO, USA), and the Colorado Children's Hospital Research Institute (Aurora, CO, USA) to K.H.P.; NIH/National Institute of Child Health and Human Development (R01 HD38466) and University of California–Irvine Alzheimer's Disease Research Center (NIH AG16573, Project 2) to J.B.; and NIH/National Center for Advancing Translational Sciences Colorado Clinical Translation and Science Institute (UL1 TR000154). Contents are the authors' sole responsibility and do not necessarily represent official NIH views.

REFERENCES

1. Roberson, E. D., and Mucke, L. (2006) 100 years and counting: prospects for defeating Alzheimer's disease. *Science* **314,** 781–784
2. De Strooper, B., and Annaert, W. (2000) Proteolytic processing and cell biological functions of the amyloid precursor protein. *J. Cell Sci.* **113**(Pt. 11), 1857–1870
3. O'Brien, R. J., and Wong, P. C. (2011) Amyloid precursor protein processing and Alzheimer's disease. *Annu. Rev. Neurosci.* **34,** 185–204
4. Hardy, J., and Selkoe, D. J. (2002) The amyloid hypothesis of Alzheimer's disease: progress and problems on the road to therapeutics. *Science* **297,** 353–356
5. Salbaum, J. M., and Ruddle, F. H. (1994) Embryonic expression pattern of amyloid protein precursor suggests a role in differentiation of specific subsets of neurons. *J. Exp. Zool.* **269,** 116–127
6. Arai, H., Higuchi, S., Matsushita, S., Yuzuriha, T., Trojanowski, J. Q., and Lee, V. M. (1994) Expression of beta-amyloid precursor protein in the developing human spinal cord. *Brain Res.* **642,** 132–136
7. Clarris, H. J., Key, B., Beyreuther, K., Masters, C. L., and Small, D. H. (1995) Expression of the amyloid protein precursor of Alzheimer's disease in the developing rat olfactory system. *Brain Res. Dev. Brain Res.* **88,** 87–95
8. Neve, R. L., Valletta, J. S., Li, Y., Ventosa-Michelman, M., Holtzman, D. M., and Mobley, W. C. (1996) A comprehensive study of the spatiotemporal pattern of beta-amyloid precursor protein mRNA and protein in the rat brain: lack of modulation by exogenously applied nerve growth factor. *Brain Res. Mol. Brain Res.* **39,** 185–197
9. Kirazov, E., Kirazov, L., Bigl, V., and Schliebs, R. (2001) Ontogenetic changes in protein level of amyloid precursor protein (APP) in growth cones and synaptosomes from rat brain and prenatal expression pattern of APP mRNA isoforms in developing rat embryo. *Int. J. Dev. Neurosci.* **19,** 287–296
10. Cataldo, A. M., Petanceska, S., Peterhoff, C. M., Terio, N. B., Epstein, C. J., Villar, A., Carlson, E. J., Staufenbiel, M., and Nixon, R. A. (2003) App gene dosage modulates endosomal abnormalities of Alzheimer's disease in a segmental trisomy 16 mouse model of down syndrome. *J. Neurosci.* **23,** 6788–6792

11. Salehi, A., Delcroix, J. D., Belichenko, P. V., Zhan, K., Wu, C., Valletta, J. S., Takimoto-Kimura, R., Kleschevnikov, A. M., Sambamurti, K., Chung, P. P., Xia, W., Villar, A., Campbell, W. A., Kulnane, L. S., Nixon, R. A., Lamb, B. T., Epstein, C. J., Stokin, G. B., Goldstein, L. S., and Mobley, W. C. (2006) Increased App expression in a mouse model of Down's syndrome disrupts NGF transport and causes cholinergic neuron degeneration. *Neuron* **51,** 29–42
12. Trazzi, S., Fuchs, C., Valli, E., Perini, G., Bartesaghi, R., and Ciani, E. (2013) The amyloid precursor protein (APP) triplicated gene impairs neuronal precursor differentiation and neurite development through two different domains in the Ts65Dn mouse model for Down syndrome. *J. Biol. Chem.* **288,** 20817–20829
13. Sabo, S. L., Ikin, A. F., Buxbaum, J. D., and Greengard, P. (2003) The amyloid precursor protein and its regulatory protein, FE65, in growth cones and synapses in vitro and in vivo. *J. Neurosci.* **23,** 5407–5415
14. Small, D. H., Nurcombe, V., Reed, G., Clarris, H., Moir, R., Beyreuther, K., and Masters, C. L. (1994) A heparin-binding domain in the amyloid protein precursor of Alzheimer's disease is involved in the regulation of neurite outgrowth. *J. Neurosci.* **14,** 2117–2127
15. Beher, D., Hesse, L., Masters, C. L., and Multhaup, G. (1996) Regulation of amyloid protein precursor (APP) binding to collagen and mapping of the binding sites on APP and collagen type I. *J. Biol. Chem.* **271,** 1613–1620
16. Kibbey, M. C., Jucker, M., Weeks, B. S., Neve, R. L., Van Nostrand, W. E., and Kleinman, H. K. (1993) beta-Amyloid precursor protein binds to the neurite-promoting IKVAV site of laminin. *Proc. Natl. Acad. Sci. U. S. A.* **90,** 10150–10153
17. Williamson, T. G., Mok, S. S., Henry, A., Cappai, R., Lander, A. D., Nurcombe, V., Beyreuther, K., Masters, C. L., and Small, D. H. (1996) Secreted glypican binds to the amyloid precursor protein of Alzheimer's disease (APP) and inhibits APP-induced neurite outgrowth. *J. Biol. Chem.* **271,** 31215–31221
18. Caceres, J., and Brandan, E. (1997) Interaction between Alzheimer's disease beta A4 precursor protein (APP) and the extracellular matrix: evidence for the participation of heparan sulfate proteoglycans. *J. Cell. Biochem.* **65,** 145–158
19. Coulson, E. J., Barrett, G. L., Storey, E., Bartlett, P. F., Beyreuther, K., and Masters, C. L. (1997) Down-regulation of the amyloid protein precursor of Alzheimer's disease by antisense oligonucleotides reduces neuronal adhesion to specific substrata. *Brain Res.* **770,** 72–80
20. Ho, A., and Sudhof, T. C. (2004) Binding of F-spondin to amyloid-beta precursor protein: a candidate amyloid-beta precursor protein ligand that modulates amyloid-beta precursor protein cleavage. *Proc. Natl. Acad. Sci. U. S. A.* **101,** 2548–2553
21. Young-Pearse, T. L., Chen, A. C., Chang, R., Marquez, C., and Selkoe, D. J. (2008) Secreted APP regulates the function of full-length APP in neurite outgrowth through interaction with integrin beta1. *Neural Dev.* **3,** 15
22. Hoe, H. S., Lee, K. J., Carney, R. S., Lee, J., Markova, A., Lee, J. Y., Howell, B. W., Hyman, B. T., Pak, D. T., Bu, G., and Rebeck, G. W. (2009) Interaction of reelin with amyloid precursor protein promotes neurite outgrowth. *J. Neurosci.* **29,** 7459–7473
23. Rice, H. C., Young-Pearse, T. L., and Selkoe, D. J. (2013) Systematic evaluation of candidate ligands regulating ectodomain shedding of amyloid precursor protein. *Biochemistry* **52,** 3264–3277
24. Qiu, W. Q., Ferreira, A., Miller, C., Koo, E. H., and Selkoe, D. J. (1995) Cell-surface beta-amyloid precursor protein stimulates neurite outgrowth of hippocampal neurons in an isoform-dependent manner. *J. Neurosci.* **15,** 2157–2167
25. Sabo, S. L., Ikin, A. F., Buxbaum, J. D., and Greengard, P. (2001) The Alzheimer amyloid precursor protein (APP) and FE65, an APP-binding protein, regulate cell movement. *J. Cell Biol.* **153,** 1403–1414
26. Song, P., and Pimplikar, S. W. (2012) Knockdown of amyloid precursor protein in zebrafish causes defects in motor axon outgrowth. *PLoS One* **7,** e34209
27. Young-Pearse, T. L., Bai, J., Chang, R., Zheng, J. B., LoTurco, J. J., and Selkoe, D. J. (2007) A critical function for beta-amyloid precursor protein in neuronal migration revealed by in utero RNA interference. *J. Neurosci.* **27,** 14459–14469
28. Allinquant, B., Hantraye, P., Mailleux, P., Moya, K., Bouillot, C., and Prochiantz, A. (1995) Downregulation of amyloid precursor protein inhibits neurite outgrowth in vitro. *J. Cell Biol.* **128,** 919–927
29. Herms, J., Anliker, B., Heber, S., Ring, S., Fuhrmann, M., Kretzschmar, H., Sisodia, S., and Muller, U. (2004) Cortical dysplasia resembling human type 2 lissencephaly in mice lacking all three APP family members. *EMBO J.* **23,** 4106–4115
30. Korte, M., Herrmann, U., Zhang, X., and Draguhn, A. (2012) The role of APP and APLP for synaptic transmission, plasticity, and network function: lessons from genetic mouse models. *Exp. Brain Res.* **217,** 435–440
31. Sosa, L. J., Bergman, J., Estrada-Bernal, A., Glorioso, T. J., Kittelson, J. M., and Pfenninger, K. H. (2013) Amyloid precursor protein is an autonomous growth cone adhesion molecule engaged in contact guidance. *PLoS One* **8,** e64521
32. Kim, J. M., Park, W. H., and Min, B. M. (2005) The PPFLMLLKGSTR motif in globular domain 3 of the human laminin-5 alpha3 chain is crucial for integrin alpha3beta1 binding and cell adhesion. *Exp. Cell Res.* **304,** 317–327
33. Tessier-Lavigne, M., and Goodman, C. S. (1996) The molecular biology of axon guidance. *Science* **274,** 1123–1133
34. Haydar, T. F., and Reeves, R. H. (2012) Trisomy 21 and early brain development. *Trends Neurosci.* **35,** 81–91
35. Reeves, R. H., Irving, N. G., Moran, T. H., Wohn, A., Kitt, C., Sisodia, S. S., Schmidt, C., Bronson, R. T., and Davisson, M. T. (1995) A mouse model for Down syndrome exhibits learning and behaviour deficits. *Nat. Genet.* **11,** 177–184
36. Tashiro, K., Sephel, G. C., Weeks, B., Sasaki, M., Martin, G. R., Kleinman, H. K., and Yamada, Y. (1989) A synthetic peptide containing the IKVAV sequence from the A chain of laminin mediates cell attachment, migration, and neurite outgrowth. *J. Biol. Chem.* **264,** 16174–16182
37. Pfenninger, K. H., Ellis, L., Johnson, M. P., Friedman, L. B., and Somlo, S. (1983) Nerve growth cones isolated from fetal rat brain: subcellular fractionation and characterization. *Cell* **35,** 573–584
38. Lohse, K., Helmke, S. M., Wood, M. R., Quiroga, S., de la Houssaye, B. A., Miller, V. E., Negre-Aminou, P., and Pfenninger, K. H. (1996) Axonal origin and purity of growth cones isolated from fetal rat brain. *Brain Res. Dev. Brain Res.* **96,** 83–96
39. Rahman, A. S., Parvinjah, S., Hanna, M. A., Helguera, P. R., and Busciglio, J. (2010) Cryopreservation of cortical tissue blocks for the generation of highly enriched neuronal cultures. *J. Vis. Exp.* **45,** 2384
40. Bottenstein, J. E., and Sato, G. H. (1979) Growth of a rat neuroblastoma cell line in serum-free supplemented medium. *Proc. Natl. Acad. Sci. U. S. A.* **76,** 514–517
41. Knoll, B., Weinl, C., Nordheim, A., and Bonhoeffer, F. (2007) Stripe assay to examine axonal guidance and cell migration. *Nat. Protoc.* **2,** 1216–1224
42. von Philipsborn, A. C., Lang, S., Bernard, A., Loeschinger, J., David, C., Lehnert, D., Bastmeyer, M., and Bonhoeffer, F. (2006) Microcontact printing of axon guidance molecules for generation of graded patterns. *Nat. Protoc.* **1,** 1322–1328
43. Pfenninger, K. H., and Maylie-Pfenninger, M. F. (1981) Lectin labeling of sprouting neurons. II. Relative movement and appearance of glycoconjugates during plasmalemmal expansion. *J. Cell Biol.* **89,** 547–559
44. Edelstein, A., Amodaj, N., Hoover, K., Vale, R., and Stuurman, N. (2010) Computer control of microscopes using microManager. *Curr. Protoc. Mol. Biol.* Chapter 14, Unit 14.20
45. Izzard, C. S., and Lochner, L. R. (1976) Cell-to-substrate contacts in living fibroblasts: an interference reflexion study with an evaluation of the technique. *J. Cell Sci.* **21,** 129–159
46. Mikule, K., Gatlin, J. C., de la Houssaye, B. A., and Pfenninger, K. H. (2002) Growth cone collapse induced by semaphorin 3A requires 12/15-lipoxygenase. *J. Neurosci.* **22,** 4932–4941
47. Curtis, A. S. (1964) The mechanism of adhesion of cells to glass. A study by interference reflection microscopy. *J. Cell Biol.* **20,** 199–215
48. Lotz, M. M., Burdsal, C. A., Erickson, H. P., and McClay, D. R. (1989) Cell adhesion to fibronectin and tenascin: quantitative measurements of initial binding and subsequent strengthening response. *J. Cell Biol.* **109,** 1795–1805

49. Limozin, L., and Sengupta, K. (2009) Quantitative reflection interference contrast microscopy (RICM) in soft matter and cell adhesion. *Chemphyschem* **10,** 2752–2768
50. Davisson, M. T., Schmidt, C., Reeves, R. H., Irving, N. G., Akeson, E. C., Harris, B. S., and Bronson, R. T. (1993) Segmental trisomy as a mouse model for Down syndrome. *Prog. Clin. Biol. Res.* **384,** 117–133
51. Busciglio, J., Pelsman, A., Wong, C., Pigino, G., Yuan, M., Mori, H., and Yankner, B. A. (2002) Altered metabolism of the amyloid beta precursor protein is associated with mitochondrial dysfunction in Down's syndrome. *Neuron* **33,** 677–688
52. Haspel, J., Friedlander, D. R., Ivgy-May, N., Chickramane, S., Roonprapunt, C., Chen, S., Schachner, M., and Grumet, M. (2000) Critical and optimal Ig domains for promotion of neurite outgrowth by L1/Ng-CAM. *J. Neurobiol.* **42,** 287–302
53. Hunter, C. L., Isacson, O., Nelson, M., Bimonte-Nelson, H., Seo, H., Lin, L., Ford, K., Kindy, M. S., and Granholm, A. C. (2003) Regional alterations in amyloid precursor protein and nerve growth factor across age in a mouse model of Down's syndrome. *Neurosci. Res.* **45,** 437–445
54. Spellman, C., Ahmed, M. M., Dubach, D., and Gardiner, K. J. (2013) Expression of trisomic proteins in Down syndrome model systems. *Gene* **512,** 219–225
55. Rumble, B., Retallack, R., Hilbich, C., Simms, G., Multhaup, G., Martins, R., Hockey, A., Montgomery, P., Beyreuther, K., and Masters, C. L. (1989) Amyloid A4 protein and its precursor in Down's syndrome and Alzheimer's disease. *N. Engl. J. Med.* **320,** 1446–1452
56. Griffin, W. S., Sheng, J. G., McKenzie, J. E., Royston, M. C., Gentleman, S. M., Brumback, R. A., Cork, L. C., Del Bigio, M. R., Roberts, G. W., and Mrak, R. E. (1998) Life-long overexpression of S100beta in Down's syndrome: implications for Alzheimer pathogenesis. *Neurobiol. Aging* **19,** 401–405
57. Engidawork, E., and Lubec, G. (2001) Protein expression in Down syndrome brain. *Amino Acids* **21,** 331–361
58. Nixon, R. A. (2007) Autophagy, amyloidogenesis and Alzheimer disease. *J. Cell Sci.* **120,** 4081–4091
59. Lemmon, V., Burden, S. M., Payne, H. R., Elmslie, G. J., and Hlavin, M. L. (1992) Neurite growth on different substrates: permissive versus instructive influences and the role of adhesive strength. *J. Neurosci.* **12,** 818–826
60. DiMilla, P. A., Stone, J. A., Quinn, J. A., Albelda, S. M., and Lauffenburger, D. A. (1993) Maximal migration of human smooth muscle cells on fibronectin and type IV collagen occurs at an intermediate attachment strength. *J. Cell Biol.* **122,** 729–737
61. DiMilla, P. A., Barbee, K., and Lauffenburger, D. A. (1991) Mathematical model for the effects of adhesion and mechanics on cell migration speed. *Biophys. J.* **60,** 15–37
62. Leeuwen, F. N., Kain, H. E., Kammen, R. A., Michiels, F., Kranenburg, O. W., and Collard, J. G. (1997) The guanine nucleotide exchange factor Tiam1 affects neuronal morphology; opposing roles for the small GTPases Rac and Rho. *J. Cell Biol.* **139,** 797–807
63. Kunda, P., Paglini, G., Quiroga, S., Kosik, K., and Caceres, A. (2001) Evidence for the involvement of Tiam1 in axon formation. *J. Neurosci.* **21,** 2361–2372
64. Vielmetter, J., Stolze, B., Bonhoeffer, F., and Stuermer, C. A. (1990) In vitro assay to test differential substrate affinities of growing axons and migratory cells. *Exp. Brain Res.* **81,** 283–287

Received for publication July 31, 2013.
Accepted for publication August 26, 2013.